Aggregation Behavior of the Antibiotic Moenomycin A in Aqueous Solution

Gabriela Lantzsch,*,† Hans Binder,† Heiko Heerklotz,† Peter Welzel,‡ and Gotthard Klose†

Institut für Experimentelle Physik I, Universität Leipzig, Linnèstrasse 5, D-04103 Leipzig, Germany, and Institut für Organische Chemie, Universität Leipzig, Talstrasse 35, D-04103 Leipzig, Germany

Received February 23, 1998. In Final Form: May 5, 1998

The aggregation behavior of the antibiotic moenomycin A (MoA) in aqueous solution under the influence of pH and ionic strength has been investigated using the fluorescent probe pyrene. Changes of the cmc between 0.03 and 0.7 mM correlate with the effective charge of MoA originating from three ionizable groups, the pK_a of which have been determined by infrared spectroscopy. The dependence of the polarity-sensitive ratio of pyrene monomer fluorescence (I_3/I_1) and the monomer-to-excimer ratio (I_{ex}/I_{mo}) on the MoA concentration were analyzed in terms of a polydispersity model. This takes into account statistical and thermodynamic aspects of detergent aggregation, electrostatic interactions between charged groups in spherical micelles, fluorescence emission properties of the probe, and their partition between water and micelles. The mean aggregation number calculated was found to be compatible with the value obtained independently by means of time-resolved fluorescence measurements. The micellization of the nonionic detergent $C_{12}E_8$ in water has been investigated in parallel as a reference. The fluorescent probe DPH has been found to be unsuitable to detect the cmc of MoA.

Introduction

The structure of micelles and their formation is related to the physicochemical problems of solubilization of hydrophobic compounds and to useful model systems of biological membrane structures. It is widely recognized that the properties of micellar solutions are determined largely by a delicate hydrophilic/hydrophobic balance introduced by the amphiphilic character of the detergent, depending on the length and structure of the hydrophobic chains on one hand and the nature of the polar headgroup on the other. Hence, factors that affect these structural units modify the aggregation behavior of the detergents as well. In particular, the cmc and the aggregation number of ionic surfactants change drastically with pH and ionic strength of the aqueous solution.[3] The most fundamental investigations on ionic surfactants were performed using amphiphilic molecules with small, singly charged headgroups such as SDS and CTAC.[4] In general, the polar heads can constitute more extended moieties with a certain number of charged groups. The question of "how micellization changes as detergent changes" is of fundamental interest to the relationship between the molecular structure and the properties of micellar systems.

We studied the self-organization of the antibiotic moenomycin A (MoA) in aqueous solution using fluorescence techniques. MoA represents an ionic amphiphilic molecule of a relatively complicated structure. It consists of a bulky headgroup containing five sugar units and a highly unsaturated, branched C_{25} lipid chain (see **1** in Figure 1). The headgroup contains three acidic functions: (i) a strongly acidic phosphoric acid diester group, (ii) a carboxylic acid group, and (iii) an enolized 1,3-diketone unit, the latter two with medium pK_a values (vide infra). Although ultracentrifugation yielded first indications of micelle formation of MoA,[5,6] details of its aggregation are unknown. We present here a systematic study of the behavior of MoA in aqueous solution at different ionic strengths and pH values as a function of the MoA concentration. The degree of dissociation of the acid groups of MoA in the aggregated state was determined by infrared spectroscopy.

The antibiotic activity of MoA is based on its inhibition of the transglycosylation reaction in the biosynthesis of the cell wall peptidoglycan of Gram-positive bacteria.[7] The knowledge of the self-aggregation properties of MoA constitutes an important aspect of studies on membrane−MoA interactions which have been shown to be of prime importance to the biological activity.[8]

Fluorescence probe techniques and, in particular, the use of the hydrophobic fluorophores pyrene and 1,6-diphenyl-1,3-hexatriene (DPH) represent standard methods for micellization studies. In the case of MoA, the application of DPH is impeded owing to specific properties of the micelles formed. The polarity-sensitive fluorescence ratio and the excimer formation of pyrene are analyzed in parallel in terms of a polydispersity model[1,2] of micelle formation. This method yields the critical micelle con-

* To whom correspondence should be addressed: (e-mail) lantzsch@rz.uni-leipzig.de; (fax) +49-341-9732479.

† Institut für Experimentelle Physik I.

‡ Institut für Organische Chemie.

(1) Tanford, C. *The Hydrophobic Effect*, 2nd ed.; Wiley: New York, 1980.

(2) Israelachvili, J. N. *Intermolecular and Surface Forces*, 2nd ed.; Academic Press: London, 1991.

(3) Clint, J. H. *Surfactant Aggregation*; Blackie: Glasgow and London, 1992.

(4) Kosswig, K.; Stache, H. *Die Tenside*; C. Hanser Verlag: München, 1993.

(5) Huber, G.; Schacht, U.; Weidenmüller, H. L.; Schmidt-Thomé, J.; Duphorn, J.; Tschesche, R. *Antimicrob. Agents Chemother.* **1965**, 737.

(6) Lenoir, D.; Tschesche, R.; Wucherpfennig, W.; Huber, G.; Weidemüller, H. L. *Antimicrob. Agents Chemother.* **1969**, 144.

(7) Welzel, P. Transglycosylase Inhibition. In *Antibiotics and Antiviral Compounds−Chemical Synthesis and Modifications*; Krohn, K., Kirst, H., Maas, H., Eds.; VCH: Weinheim, 1993.

(8) Kempin, U.; Hennig, L.; Welzel, P.; Marzian, S.; Müller, D.; Fehlhaber, H.-W.; Markus, A.; van Heijenoort, Y.; van Heijenoort, J. *Tetrahedron* **1995**, *51*, 8471.

S0743-7463(98)00214-5 CCC: $15.00
Published on Web 07/03/1998

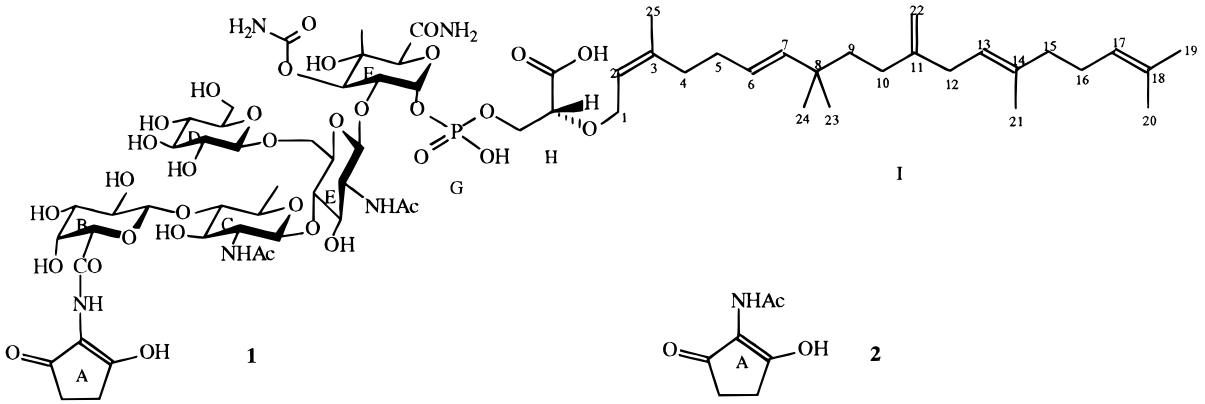

Figure 1. Chemical structure of moenomycin A (**1**) and of model compound *N*-(2-hydroxy-5-oxocyclopent-1-enyl)acetamide (**2** and **A**). The letters B−F indicate the sugar moieties, G is the phosphate group, H is the glyceric acid group, and I is the hydrocarbon part of the MoA molecule.

centration (cmc), the mean aggregation number, the micelle size distribution, and information about the distribution of the probe molecules between the aqueous and micellar phases. To evaluate the method and for direct comparison with MoA we performed measurements using the nonionic detergent $C_{12}E_8$ in aqueous solution as a reference system.

Materials and Methods

Materials. MoA (Figure 1) was obtained from Hoechst, Marion Roussel and purified by RP_{18} HPLC, elution with methanol−water (65:35). The oligo(ethylene glycol) dodecyl ether $C_{12}EO_8$ was purchased from Nikko Chemicals Co. The fluorescent probes pyrene and DPH were obtained from Serva. Pyrene was recrystallized twice from ethanol before use, and DPH was utilized without further purification. All other reagents used were products of Fluka and ACROS. Phosphate buffer (KH_2PO_4, Na_2HPO_4) and the universal buffer (citric acid, H_3BO_3, $KHSO_4$, diethylbarbituric acid) were prepared with tridistilled water and used at various pH values adjusted between 2.6 and 9.6. The model compound *N*-(2-hydroxy-5-oxocyclopent-1-enyl)acetamide (**2**, see Figure 1) was prepared as described in ref 9. It was attached for UV−visible staining.

Adjustment of pH, pD, and Ionic Strength. MoA was dissolved in water or buffer in concentrations up to 4 mM. To exclude any specific buffer effects on MoA, the experiments were performed using two different buffer systems: phosphate buffer and the universal buffer (vide supra). The pH values were adjusted with a Präcitronic MV 870 pH meter equipped with a Mettler Toledo glass electrode. The pD values were calculated using the empirical relationship pD = "pH meter reading" + 0.4 (T = 25 °C).[10] The ionic strengths of the buffer solutions (see below) were determined from the concentrations of the ions, C_i, assuming complete dissociation for the cations Na^+ and K^+ and a dissociation equilibrium according to the Henderson−Hasselbalch equation for the anions. In some cases, the ionic strength of the buffer was increased by addition of NaCl.

For infrared measurements, **1** and **2** were dissolved in H_2O or D_2O (15 and 50 mM, respectively). The pH or pD values were varied by adding appropriate amounts of 5 M solutions of NaOH (NaOD) or HCl (DCl) to the sample solution.

Fluorescence Measurements. Steady-state fluorescence measurements were performed on a CD900 spectrofluorometer (Edinburgh Instruments) using 1.5-nm slits for the excitation and the emission monochromators. Time-resolved measurements were carried out at the CD900 instrument working in the time-correlated single-photon-counting mode or at a LIF 200 system, equipped with an MCP photomultiplier C2773 (Hamamatsu) and a real-time oscilloscope 54720A (Hewlett-Packard) for detecting the nanosecond time decay (250-ps resolution). In the latter case, a nitrogen laser (λ = 337 nm, 20 Hz) was used for excitation. The temperature was adjusted using piezoelectric elements.

(a) DPH. Appropriate amounts of the stock solution of DPH (in tetrahydrofuran) were added to the aqueous phase and stirred (1−2 h) in the dark. This procedure was sufficient to remove the tetrahydrofuran as indicated in terms of the fluorescence intensity of DPH at 430 nm (λ_{ex} = 360 nm).

After stepwise additions of 4−10 mM $C_{12}EO_8$ or MoA stock solutions, respectively, the samples were stirred for 15 min for equilibration and then the fluorescence spectra were recorded. The measurements were carried out at 25 °C.

(b) Pyrene. Stock solutions of pyrene (in chloroform−methanol, 3:1 v/v) and of the detergent (in methanol) were mixed in a molar ratio 1:50 (r_{PY} = 0.02), dried under vacuum, dissolved in the respective aqueous solution (see below), and stored overnight at 4 °C. The dependence of the detergent concentration, D_t, was measured by means of stepwise dilution of the original sample solution (4 mM). The samples were thermostated at 25 °C and stirred for at least 10 min before each measurement in order to equilibrate the system. Pyrene fluorescence was excited at 320 nm rather than at 337 nm in order to avoid the spectral overlap between the corresponding Raman band of water (382 nm at λ_{ex} = 337 nm) and the pyrene monomer fluorescence. The polarity sensitive ratio I_3/I_1 was based on the emission intensities at 372 (I_1) and 383 nm (I_3) and the excimer-to-monomer fluorescence intensity ratio of pyrene, I_{ex}/I_{mo}, was taken at 480 (I_{ex}) and 393 nm (I_{mo}). Overlapping contributions of the excimer fluorescence were subtracted from the monomer intensities.

Infrared Measurements. Infrared spectra with a resolution of 2 cm^{-1} were measured in the transmission mode using a BioRad FTS-60a Fourier transform infrared spectrometer. The appropriate amounts of the sample solution were placed in a thermostated liquid cell with two ZnSe windows separated by a 25-μm spacer. Absorbance spectra of the sample were calculated using the spectrum of the solvent as background. Typically, 256 scans were accumulated. Deuterated MoA and deuterated **2** (exchangeable protons) were used for measurements in D_2O.

Theory

Polydispersity and Aggregation Number. In a polydisperse micellar solution, the mole fraction, X_m^N, of the detergent situated in micelles of the aggregation number, N, is given by[2]

$$X_m^N \equiv \frac{D_m^N}{D_t + W} = (X_w)^N N \exp\left(-\frac{N\Delta\mu_0^N}{RT}\right) \qquad (1)$$

R, T, and $\Delta\mu_0^N$ denote the gas constant, the absolute temperature, and the difference of the standard chemical potential of the detergent upon transfer from water into the micelle of size N, respectively. D_m^N represents the molar concentration of the detergent residing in micelles of size N, D_t, the total detergent concentration, and W the

(9) Kempin, U.; Hennig, L.; Knoll, D.; Welzel, P.; Müller, D.; Markus, A.; van Heijenoort, J. *Tetrahedron* **1997**, *53*, 17669.

(10) Fife, T. H.; Bruice, T. C. *J. Phys. Chem.* **1961**, *65*, 1079.

water concentration. X_w denotes the molar fraction of detergent remained in water. In the case of the high dilution used in this work ($W \approx 55.5$ mol/L $\gg D_t$), the mole fractions of the micellar and monomeric detergent, X_m and X_w, respectively, are

$$X_m = \sum_{N=2}^{\infty} X_m^N \approx D_m/W \quad \text{and} \quad X_w \approx D_w/W \tag{2}$$

Hence, using eq 1 one can calculate the size distribution of the micelles $X_m^N(N)$, $N > 2$ for chosen values of X_w and $\Delta\mu_0^N$ (see below). The sum over the size distribution yields X_m. The corresponding D_t is determined by the balance of the concentrations of micellar and aqueous detergent, D_m and D_w; i.e., $D_t = D_m + D_w = W(X_m + X_w)$ (cf. eq 2).

The mean aggregation number, $\bar{N}$, is given by

$$\bar{N} = \frac{1}{X_m}\sum_{N=2}^{\infty} N X_m^N \tag{3}$$

Standard Chemical Transfer Potential as a Function of the Aggregation Number, *N*. According to the idea of opposing interfacial forces, the micelles are stabilized by attractive and repulsive forces giving rise to a minimum of the interfacial free energy and thus to an optimum interfacial area per molecule, a_0. $\Delta\mu_0^N$ can be expressed as a function of a_N, the surface area per molecule in micelles of size N,[1] i.e.:

$$\Delta\mu_0^N = 2\gamma a_0 + \frac{\gamma}{a_N}(a_N - a_0)^2 + W_N \tag{4}$$

where γ is the surface tension. Contributions originating from the hydrophobic effect and steric interactions account for the first two terms of eq 4. In the case of ionic detergents, the electrostatic interaction energy, W_N, can be estimated in terms of the approximation that all charged groups are located on a spherical surface of radius R_N,[1] i.e.:

$$W_N = q^2 \frac{R_N}{a_N}\frac{1}{2\epsilon} f, \quad \text{with} \quad f = \frac{\left(1 + \frac{r_i}{r_D}\right)}{\left(1 + \frac{R_N}{r_D} + \frac{r_i}{r_D}\right)} \tag{5}$$

where q and ϵ denote the charge per molecule and the dielectric constant of the electrolyte, respectively. The electrostatic scaling factor, f, depends on r_i, the average radius of mobile ions dissoluted in the surrounding electrolyte ($r_i \approx 0.2$ nm) and r_D, the Debye−Hückel length. The latter is given by

$$r_D = \sqrt{\epsilon kT/2N_A e^2 I} \quad \text{with} \quad I = \frac{1}{2}\sum_i C_i |z_i|^2 \tag{6}$$

where k denotes the Botzmann constant, N_A, Avogadro's number, and e the elementary charge. The ionic strength, I, depends on the concentration, C_i, and the charge number, z_i, of all ions in the aqueous solution (see Materials and Methods).

For spherical micelles, simple geometric considerations yield relations between the molecular surface area requirement, a_N, and the radius of the hydrophobic core, r_N, on one hand, and the aggregation number, N, and the hydrophobic volume per molecule, v, which is assumed to be incompressible (i.e. v = const), on the other hand,

$$a_N = \left(\frac{36\pi}{N}v^2\right)^{1/3} \quad \text{and} \quad r_N = \left(\frac{3N}{4\pi}v\right)^{1/3} \tag{7}$$

If the hydrophobic tails of the detergent molecules consist of hydrocarbon chains of n_h methylene groups, the maximum length and the volume of the hydrophobic moiety can be estimated by[1]

$$l_{max} \approx (0.15 + 0.1265 n_h)\ \text{nm}$$
$$v \approx (27.4 + 26.9 n_h) \times \text{nm}^3 \tag{8}$$

Note, that l_{max} constitutes an upper limit of r_N and, consequently, determines a maximum aggregation number compatible with a spherical geometry:

$$N_{max} = 4\pi l_{max}/3v \tag{9}$$

Pyrene Fluorescence Intensity in Micellar Dispersions. In micellar dispersions, the hydrophobic fluorophore pyrene is located preferentially within the micelles.[11,12] However, a residual number of fluorophores usually remains dissolved within the aqueous phase in the monomeric form up to a concentration of $Py_w^{crit} \approx 1-2$ μM. Probe molecules exceeding this limit form aggregates (microcrystals/micelles) showing a nonnegligible excimer fluorescence. The fluorescence intensity in micellar dispersions, I_i, originates from pyrene solubilized within the micellar and aqueous phases in fractions of f_m and $f_w = (1 - f_m)$ of the total pyrene concentration $Py_t = r_{Py}{\cdot}D_t$, i.e.,

$$I_i = (I_i^m f_m + I_i^w(1 - f_m)), \quad i = 1, 3, \text{mo,ex} \tag{10}$$

I_i^m and I_i^w denote the fluorescence intensities in the case where all pyrene molecules would be located in the micellar and water phases, respectively. Using eq 10, the following general equation of the intensity ratios (I_3/I_1) and (I_{ex}/I_{mo}) can be derived

$$\frac{I_i}{I_j} = \frac{\frac{I_i^m}{I_j^m} + \frac{1 - f_m}{f_m}\frac{I_i^w}{I_j^w}k_j}{1 + \frac{1 - f_m}{f_m}k_j}, \quad i = 3, \text{ex} \quad \text{and} \quad j = 1, \text{mo} \tag{11}$$

$k_j = I_j^w/I_j^m$, the ratio of the intensities of the respective vibronic bands of pyrene monomer fluorescence in an aqueous to that in a hydrophobic environment, is estimated as $k_1 \approx 0.6$ and $k_{mo} \approx 0.44$ using reference samples of pyrene dissolved in water and $C_{12}EO_8$, respectively. For the polarity-sensitive ratio of pyrene in water we measured $I_3^w/I_1^w = 0.55$. The excimer-to-monomer ratio was $I_{ex}^w/I_{mo}^w = 0$ for aqueous pyrene concentrations below Py_w^{crit}. Beyond Py_w^{crit} we estimated $I_{ex}^w/I_{mo}^w = m = 0.06-0.1$ in the fitting procedures (see below).

At low pyrene concentrations ($Py_t \ll D_t \ll W$), the mole fractions of pyrene in the micellar and the aqueous phases are given to a good approximation by

(11) Kalyanasundaram K.; Thomas, J. K. *J. Am. Chem. Soc.* **1977**, *99*, 2039.

(12) Atik, S. S.; Nam, M.; Singer, L. A. *Chem. Phys. Lett.* **1979**, *67*, 75.

$$X_{\mathrm{py,m}} = \frac{f_{\mathrm{m}}\mathrm{Py_t}}{f_{\mathrm{m}}\mathrm{Py_t} + D_{\mathrm{m}}} \approx \frac{f_{\mathrm{m}}\mathrm{Py_t}}{D_{\mathrm{m}}} \quad \text{and}$$

$$X_{\mathrm{py,w}} = \frac{(1 - f_{\mathrm{m}})\mathrm{Py_t}}{(1 - f_{\mathrm{m}})\mathrm{Py_t} + W} \approx \frac{(1 - f_{\mathrm{m}})\mathrm{Py_t}}{W} \quad (12)$$

respectively. Using these definitions, the fraction of pyrene located within the micelles, f_{m}, can be estimated by assuming a partition behavior of the fluorophore with the partition coefficient, P:

$$P = \frac{X_{\mathrm{py,m}}}{X_{\mathrm{py,w}}} \approx \frac{f_{\mathrm{m}}}{(1 - f_{\mathrm{m}})X_{\mathrm{m}}} \quad (13)$$

yielding

$$f_{\mathrm{m}} \approx \frac{PX_{\mathrm{m}}}{1 + PX_{\mathrm{m}}} \quad (14)$$

We assume that the polarity in the hydrophobic core of the micelles is not affected by the fluorescent probe and furthermore does not depend on the aggregation number. The excimer-to-monomer intensity ratio, $I^{\mathrm{m}}_{\mathrm{ex}}/I^{\mathrm{m}}_{\mathrm{mo}}$, on the other hand depends on the pyrene concentration in the micelles owing to the bimolecular nature of excimer formation. In a crude approximation, we assume direct proportionality between $I_{\mathrm{ex}}/I_{\mathrm{mo}}$ and the local concentration of pyrene monomers which is given roughly by $\bar{n}/\bar{N}$, i.e.

$$I^{\mathrm{m}}_{\mathrm{ex}}/I^{\mathrm{m}}_{\mathrm{mo}} \approx K(\bar{n}/\bar{N}) \quad (15)$$

The mean number of pyrene molecules per micelle, $\bar{n}$, is directly related to the mean aggregation number, $\bar{N}$,

$$\bar{n} \approx f_{\mathrm{m}}\mathrm{Py_t}\bar{N}/D_{\mathrm{m}} \quad (16)$$

In the frame of this approximation the intensity ratio $I^{\mathrm{m}}_{\mathrm{ex}}/I^{\mathrm{m}}_{\mathrm{mo}}$ transforms to

$$I^{\mathrm{m}}_{\mathrm{ex}}/I^{\mathrm{m}}_{\mathrm{mo}} \approx K(f_{\mathrm{m}}\mathrm{Py_t}/D_{\mathrm{m}}) \quad (17)$$

The proportionality constant, K, depends on the rate constants of excimer fluorescence, on the natural lifetimes of monomers and excimers, on the diffusibility of pyrene in the host matrix, and on a geometrical factor.[13] In the present work, K was used as a free adjustable parameter without further specification.

Summarizing, we state that the intensity ratios I_3/I_1 and $I_{\mathrm{ex}}/I_{\mathrm{mo}}$ can be obtained by eqs 11 and 15 using the fraction of pyrene situated in micelles (cf. eq 14) at a micellar detergent concentration, X_{m}, existing in the polydisperse micellar dispersion at a given detergent concentration, D_{t}. In other words, one can calculate the corresponding fluorescence intensity ratios as a function of D_{t} using the polydispersity model (cf. eqs 1−3) referring to a particular N-dependent chemical transfer potential difference (eq 4).

Results

Dissociation Equilibria of the Enol, Carboxyl, and Phosphate Groups of MoA: FTIR Measurements. The dissociation equilibria of the glyceric acid carboxyl, of the phosphate group, and of the enolized β-diketone unit A of MoA and of model compound **2** (cf. Figure 1) in D_2O and, as far as possible, in H_2O were investigated by means of FTIR.

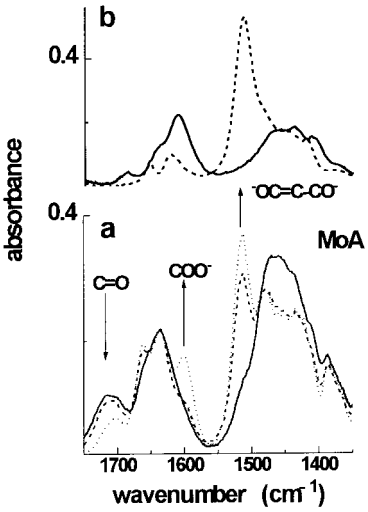

Figure 2. Infrared spectra of MoA (a) and of **2** (b) dissolved in D_2O at different pD. (a), pD = 3.5 (solid line), 5.6 (dashed), and 8.9 (dotted); in (b), 1.8 (solid) and 9.8 (dashed). Selected bands are assigned within the figure. Changes of absorbance with increasing pD are indicated by arrows.

Infrared spectra of MoA dissolved in D_2O (15 mM) are recorded at different pD values. Considerable spectral changes are observed in the range 1750−1450 cm^{-1}, where upon increasing the pD a new absorption band appears at 1600 cm^{-1} (Figure 2a) which can be assigned to the antisymmetric stretching mode of the COO^- group, $\nu_{\mathrm{as}}(COO^-)$. The increase of this band is accompanied by the parallel decrease of the broad band centered around 1710 cm^{-1} which originates from the stretching vibration of the C═O double bond, ν(C═O).

A second intense absorption band appears at 1513 cm^{-1} with increasing pD (Figure 2a). An identical peak was observed in the IR spectrum of the model compound **2**, which was examined separately under similar conditions (Figure 2b). This absorption band can be assigned to the antisymmetric stretching vibration of the conjugated O═C−C═C−O^- fragment resulting from OD dissociation.[14]

On the basis of these assignments, one can attribute the spectral changes observed to the increasing ionization of the carboxyl and enol groups with increasing pD. The degree of dissociation of both moieties, α_{carb} and α_{enol}, was determined by means of the integrated and normalized absorbance of the corresponding bands (Figure 3). The apparent pK_{a} is defined as the pD value of the inflection point (50% conversion). We obtained pK_{a}(COOD) = 6.1 ± 0.1 and pK_{a}(OCCCOD) = 4.6 ± 0.1 for the carboxyl and enol groups of MoA, respectively.

Repeating the infrared investigations with MoA dissolved in H_2O instead of D_2O, we established an almost identical appearance and increase of the band at 1513 cm^{-1}. The quantitative analysis yielded pK_{a}(OCCCOH) = 3.8 ± 0.1, i.e., a value diminished by $\Delta pK_{\mathrm{a}} = 0.8 \pm 0.2$ in comparison with that of the deuterated form, pK_{a}-(OCCCOD). A difference of 0.63 ± 0.07 between pK_{a} data measured in D_2O and H_2O was reported previously.[15]

Unfortunately, the absorption bands of the $\nu_{\mathrm{as}}(COO^-)$ and ν(C═O) modes cannot be analyzed in the aqueous system owing to the strong absorbance of the ν_2 vibration of water appearing in the 1600−1720-cm^{-1} range. Using

(13) Birks, J. B.; Dyson, D. J.; Munro, I. H. *Proc. R. Soc.* **1963**, *A275*, 575.

(14) Junge H.; Musso, H. *Spectrochim. Acta* **1968**, *24A*, 1219.

(15) Dagnall, S. P.; Hague, D. N.; McAdam M. E.; Moreton, A. D. *Chem. Soc., Faraday Trans. 1* **1985**, *81*, 1483.

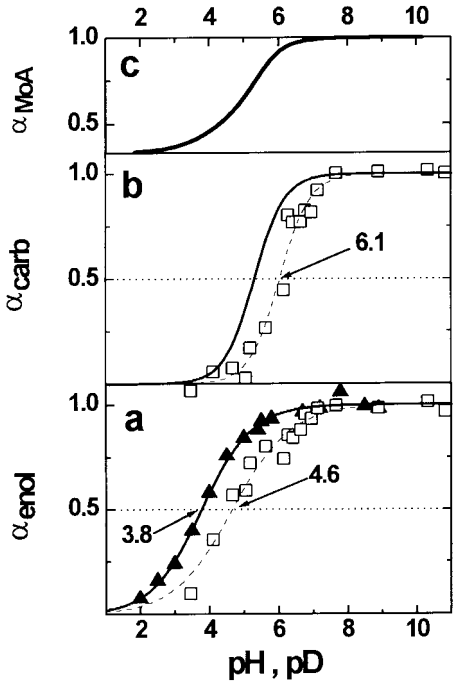

Figure 3. Degree of dissociation of the enol (a) and of the carboxyl (b) groups of MoA as a function of pH and pD. The experimental points represent the normalized, integrated absorbance of the $\nu_{as}(OCCCO^-)$ (a) and $\nu_{as}(COO^-)$ bands (b) of MoA dissolved in D_2O (open symbols, cf. Figure 2) and H_2O (solid). The lines are fits using a Boltzmann-type function. The numbers give the corresponding pK_a values. The solid curve in (b) refers to H_2O. It was obtained by shifting the curve corresponding to D_2O by pK_a(COOH) − pK_a(COOD) = −0.8. Part c shows the mean degree of dissociation of the phosphate, enol, and carboxyl groups of MoA in water. It was calculated from the superposition of the respective fitting functions (OCCCOH and COOH) by assuming that POO^- is dissociated completely at pH > 2.5.

the difference $\Delta pK_a = 0.8$ established experimentally, one obtains pK_a(COOH) = 5.3 for the dissociation of the carboxyl group of MoA.

The phosphate group represents the third charged moiety in MoA. An intense absorption band at 1225 cm^{-1} can be attributed to the antisymmetric stretching vibration of the PO_2^- group, $\nu_{as}(PO_2^-)$. It already exists at the smallest pH investigated and shows no significant modifications upon increasing pH (data not shown). We conclude that the phosphate group is deprotonated over the entire pH range used, and thus, its degree of dissociation always equals unity, $\alpha_{phos} = 1$.

Summarizing, we obtain the overall degree of dissociation of MoA as the arithmetic mean $\alpha_{MoA}(pH) = (\alpha_{carb}(pH) + \alpha_{enol}(pH) + \alpha_{phos})/3$ displayed in Figure 3c. $\alpha_{carb}(pH)$ and $\alpha_{enol}(pH)$ denote the sigmoidal functions fitted to the experimental data (Figure 3a,b).

The dissociation equilibria studied correspond to relatively concentrated aqueous solutions (15 mM) where the MoA molecules are expected to assemble into aggregates. The intrinsic pK_a^0(COOH) of a free glyceric acid, which represents the chemical compound linking the hydrophobic lipid chain and the bulky headgroup, was determined to be 3.6.[16] This value is clearly smaller than 5.3 measured in the MoA sample. Two effects must be considered to account for this fact. At the one hand, the carboxyl group of aggregated MoA is buried within the micelles and therefore somewhat screened from the bulk water phase.

(16) Ostwald, W. *Z. Phys. Chem. 3* **1889**, *170*, 418.

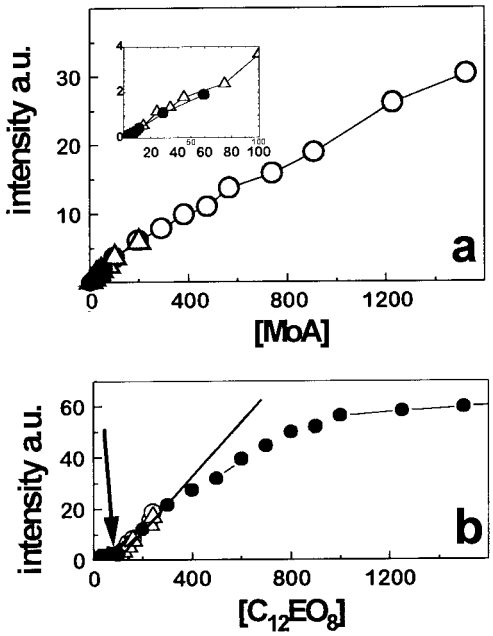

Figure 4. Fluorescence intensity of DPH as a function of detergent concentration (in μM): MoA at pH = 6.8 and I = 125 mM (a) and $C_{12}EO_8$ (b). DPH concentrations are 5 nM (●, in part a); 1 μM (△), 5 μM (○), and 10 μM (●, in part b). The inset in (a) enlarges the range of small MoA concentrations. The arrow in (b) indicates the cmc.

On the other hand, the local H^+ concentration near a negatively charged surface is increased relative to the bulk value according to the Boltzmann equation.

A negligible pK_a shift was obtained for the enol group in **1** when compared with **2**. pH titration and infrared spectral analysis of an aqueous solution of **2** yielded pK_a^0(OCCCOH) = 3.5, well in agreement with the previously published value (3.7).[17] A pK_a^0 of 3.8 was measured for the enol group in MoA. This observation can be rationalized by assuming that the enol group of MoA is localized in the outer part of the polar headgroup of MoA. In the micelles it is expected to remain strongly exposed to the water phase and, thus, to possess an environment similar to the dissolved **2**.

Concentration-Dependent Aggregation: Steady-State Fluorescence Measurements. (a) DPH. Recent NMR investigations[18] indicate a cmc of MoA in aqueous solution at ~0.7 mM. To confirm this finding by fluorescence investigations we used the hydrophobic fluorescent probe DPH, which is well suited to detect the aggregation of detergents because its quantum yield in the hydrophobic core of a micelle exceeds that in water by more than 2 orders of magnitude.[19] The DPH fluorescence intensity, I_f, of an aqueous MoA/DPH solution increases, however, nearly linearly with increasing MoA concentration, [MoA], showing no indications of a cmc (Figure 4a). Note, that this peculiar behavior of the MoA sample cannot be understood by the existence of a cmc below the smallest concentration used in the experiments because also no saturation of I_f was observed.

For comparison we performed analogous measurements using the nonionic detergent $C_{12}E_8$ with a well-known cmc. A significant fluorescence intensity appears at the cmc

(17) Tschesche, R.; Blumbach, J.; Welzel, P. *Liebigs Ann. Chem.* **1973**, 407.

(18) Hennig, L.; Findeisen, M.; Welzel, P. *Magn. Reson. Chem.*, submitted.

(19) Chattopadhyay A.; London, E. *Anal. Biochem.* **1983**, *22*, 408.

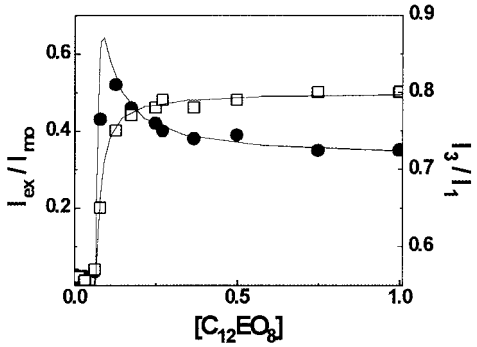

Figure 5. Intensity ratios of pyrene fluorescence, I_3/I_1 (□, right ordinate) and I_{cy}/I_{mo} (●, left ordinate), as a function of the $C_{12}E_8$ concentration (in mM). The lines represent fits using the polydispersity model (see text).

(84 μM) (cf. cmc values in refs 20−23). The subsequent almost linear increase of the intensity, I_f, vs $[C_{12}EO_8]$ is caused by the progressive partition of the fluorophore into the detergent aggregates. For $[C_{12}EO_8] > 800$ μM, the DPH molecules are almost completely located within micelles and I_f levels off.

Interestingly, the DPH fluorescence intensity of a MoA solution (1600 μM) increases more than 2-fold if one adds $C_{12}E_8$ (300 μM) to the sample. Thus, the quite different fluorescence properties of DPH in aqueous systems of $C_{12}E_8$ and MoA should be attributed to marked differences of the aggregation behavior and of the physicochemical properties of the micelles (e.g., size, polarity) formed by the nonionic and the ionic detergents. In particular, we suggest that the presence of C=C double bonds in the hydrocarbon chain of MoA restricts the conformational freedom of the chains for segmential motions and increases the polarity within the hydrophobic core of the micelles when compared with micelles of surfactants with saturated hydrocarbon chains. Both effects are expected to reduce partition of DPH into the micelles. The rodlike DPH molecules are possibly more strongly affected by steric restrictions imposed by the double bonds than the disklike pyrene molecules. Moreover, the extended, hydrophilic sugar moieties possibly promote the temporary invasion of water molecules into the hydrophobic core and thus increase the local polarity and, as a consequence, decrease the quantum yield of DPH fluorescence. Note, that the definition of the polar/apolar interface seems to be much more vague for MoA aggregates than for $C_{12}E_8$. In addition, the appearance of small premicellar aggregates (trimers,tetramers, ...) can cause an initial increase of the DPH fluorescence as observed.

(b) Pyrene. The typical behavior of the pyrene fluorescence ratios upon micelle formation is illustrated by Figure 5 for the $C_{12}EO_8$ system. Whereas no excimers are formed below the cmc, the pyrene is accumulated in the first few micelles appearing which gives rise to a considerable peak of I_{ex}/I_{mo}. Note, that the total probe-to-detergent ratio is fixed in the experiments. As a consequence, the mean number of probe molecules per micelle controlling the excimer formation levels off when the aqueous detergent fraction becomes negligible. The polarity sensitive ratio jumps from $I_3/I_1 \approx 0.55$ being typical for an aqueous environment to 0.85, the characteristic value for pyrene in micelles (SDS, 0.8−0.9;[24] Brij 35, 0.85;[11] Triton X-100, 0.76[11]). The considerable variations in I_3/I_1 and I_{ex}/I_{mo} data reflect micelle formation in the concentration range 60−80 μM in agreement with the results of DPH measurements.

Figure 6 shows the pyrene fluorescence intensity ratios I_3/I_1 and I_{ex}/I_{mo} as a function of the MoA concentration for a set of pH values (a) and ionic strengths (b). We note that the plots exhibit the same principle behavior as shown for $C_{12}EO_8$. In contrast to the DPH data, the pyrene experiments suggest the existence of a cmc for MoA and a micellar core polarity similar to $C_{12}EO_8$. Obviously pyrene is more suited than DPH for a quantitative analysis of the aggregation behavior of MoA.

As expected, the apparent cmc of MoA shifts to bigger values if one increases the pH or decreases the ionic strength, because both tendencies strengthen the Coulombic repulsion between the molecules. Namely, the increase of pH has been found to increase the net charge of MoA. With increasing I, the charges are progressively screened by counterions.

Data Analysis in Terms of the Polydispersity Model. According to the model outlined in the Theory section, the concentration dependencies of the intensity ratios I_3/I_1 and I_{ex}/I_{mo} can be described using one parameter set (q, a_0, γ, P, K, m) for each external condition (pH, ionic strength). K and m specify the excimer formation and thus apply only to I_{ex}/I_{mo}.

Let us start with the nonionic detergent $C_{12}E_8$, which is assumed to form spherical micelles[25] with a mean aggregation number $N = 70 \pm 5$ (see below). The experimental data were fitted fairly well using $q = 0$, $a_0 = 0.63$ nm^2, $\gamma = 43$ mJ m^{-2}, $P = 2.5 \times 10^6$, $K = 0.35$, $m = 0$ (see Figure 5, lines). The surface tension $\gamma = 43$ mJ m^{-2} is reasonable considering the range 25−50 mJ m^{-2} reported for amphiphilic aggregates.[2] $m = 0$ was chosen because the aqueous pyrene concentration never exceeds Py_w^{crit}. The optimum area per molecule, $a_0 = 0.63$ nm^2, refers to spherical micelles of the maximum radius, $r = l_{max}$ corresponding to an alkyl chain length $n_h = 12$ (see eqs 7 and 8). This point will be discussed below. A systematic variation of the model parameters shows that the onset of the micelle formation depends sensitively on the surface tension, γ, whereas the partition coefficient of pyrene, P, determines the sharpness of the transition (cf. Figure 7, parts P and γ). Note, that the curves drawn in Figure 7 refer to a constant ratio pyrene/detergent, r_{Py}; i.e., the amount of pyrene increases to the same extent as the detergent. Consequently, a larger number of pyrene molecules can concentrate within the aggregates if micellization starts at higher detergent concentrations. As a result, the maximum value of I_{ex}/I_{mo} increases with increasing cmc or, alternatively, a I_{ex}/I_{mo} maximum already appears at smaller P values.

To describe the aggregation behavior of the ionic detergent, the net charge of MoA, $q = ze > 0$, enters the fitting algorithm. It gives rise to a nonnegligible contribution to the chemical transfer potential (eq 4). In a first step, we optimized the parameter set by variation of γ, P, K, and m in order to fit the data measured at the smallest pH, 2.6. The charge number $z = -1$ corresponds to the dissociated phosphate group only (see Figure 3c). For the hydrophobic volume per molecule, we used $v_h = 0.673$ nm^3, which corresponds to that of a saturated hydrocarbon chain with $n_h = 24$ carbons (e.g., eq 8). Furthermore, we

(20) Heerklotz, H.; Lantzsch, G.; Binder, H.; Klose G.; Blume, A. *J. Phys. Chem.* **1996**, *100*, 6764.
(21) Shoji, N.; Ueno M.; Meguro, K. *J. Am. Oil Chem. Soc.* **1978**, *53*, 165.
(22) Rosen M. J.; Cohen, A. W.; Dahanayake, M.; Hua, X. *J. Phys. Chem.* **1982**, *86*, 541.
(23) Corti M.; Degiorgio, V. *J. Phys. Chem.* **1981**, *85*, 1443.
(24) Siemiarczuk A.; Ware, W. R. *Chem. Phys. Lett.* **1990**, *167*, 263.
(25) Nilsson, P.-G.; Wennerström H.; Lindman, B. *J. Phys. Chem.* **1983**, *87*, 1377.

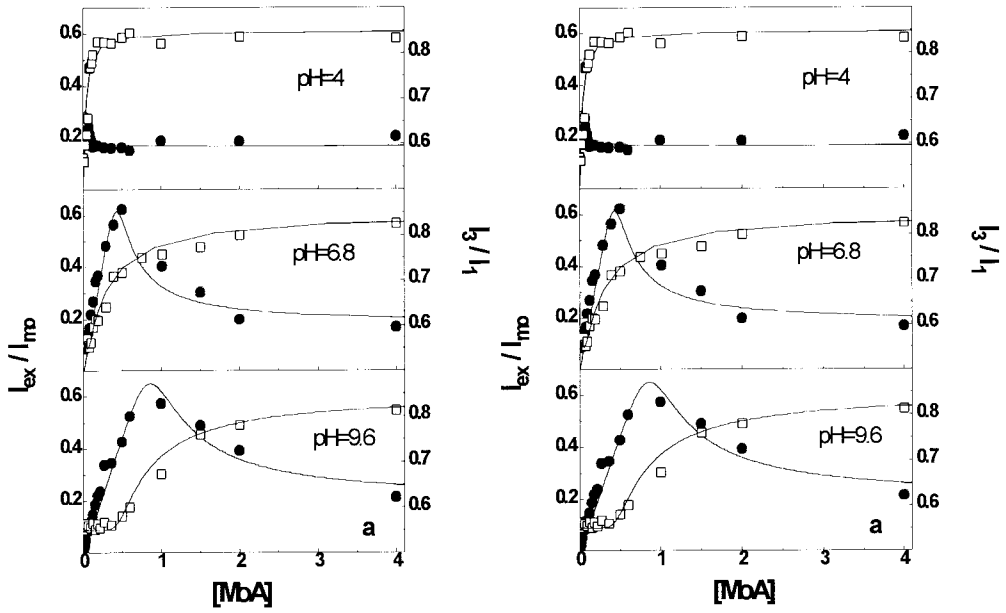

Figure 6. Intensity ratios of pyrene fluorescence, I_3/I_1 (□, right ordinate) and I_{cy}/I_{mo} (●, left ordinate), as a function of the MoA concentration (in mM) at different pH values (a, $I = 50-100$ mM) and ionic strengths (b, pH = 6.8). The corresponding pH (a) and I (b) values are indicated in the figures. The lines represent fits using the polydispersity model (see text for explanation).

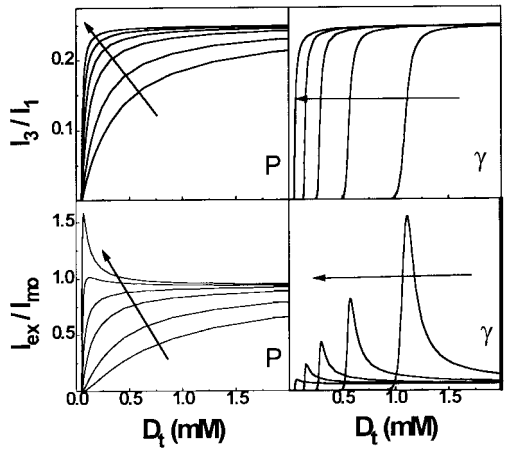

Figure 7. Theoretical I_3/I_1 (above) and I_{ex}/I_{mo} (below) curves as a function of total detergent concentration upon systematic variation of the model parameters of the polydispersity model P (left) and γ (right). The basis parameter set is $q = 0$, $a_0 = 0.63$ nm^2, $\gamma = 43$ mJ m^{-2}, $p = 2.5 \times 10^6$, $m = 0$, and $T = 25$ °C. Parameter variation refers to $P = (0.1, 0.2, 0.5, 2, 4) \times 10^6$ and $\gamma = 32, 34, 36, 38, 41$ (in direction of the arrows).

assume for a rough estimation that the charged groups are located at the hydrophobic/hydrophilic interface; i.e., we assumed $R_N = r_N$ in eq 5. For the fit of the fluorescence data measured at all other pH values and ionic strengths, the parameters, z, P, K, and m were varied whereas $\gamma = 41$ mJ m^{-2}, the optimum value obtained at pH = 2.6, was held fixed. Hence, we assume that the modification of the aggregation of MoA in comparison with its properties at pH = 2.6 is caused solely by the variation of the electrostatic interactions between the molecules. Optimal fits are drawn by lines in Figure 6 and the corresponding parameters are listed in Table 1. A constant value of the optimum area per molecule, $a_0 = 0.9$ nm^2, was used in all calculations. The variation of a_0 by ±0.1 nm^2 shifts the resulting parameters slightly in a systematic fashion.

The polydispersity model does not use the cmc as an explicit parameter. The cmc data listed in Table 1 represent the aqueous detergent concentration, D_w, at which 50% of the detergent is within the aggregates ($X_m = 0.5$). Note, that this value coincides practically with the concentration, D_t, at which the experimental I_3/I_1 data start to increase. Hence, this onset point of the transition can be determined alternatively by linear extrapolation of the basis line and the raising part of the experimental I_3/I_1 dependencies.

Table 1. Fit Parameters, *z*, *P*, and *K* of the Intensity Ratios I_3/I_1 and I_{ex}/I_{mo} in the MoA Solutions Investigated

exp conditions		optimal fit parameters			micelle properties		
pH[a]	I (mM)	z_{fl}	P ($\times 10^6$)	K	$\bar{N}$[b]	$\Delta\mu_0^N$ (kJ mol^{-1})[c]	cmc (mM)[d]
2.6	35	1	3.5	9	36	−36	0.019
4	51	1.28	4	8	29	−32	0.062
6.8	79	1.63	0.4	14	24	−28.5	0.26
9.6	95	1.8	0.1	18	21	−26	0.65
6.8	79	1.84	0.15	10	21	−25.5	0.65
6.8	154	1.86	0.5	12	22	−27	0.43
6.8	316	1.67	1	11	29	−32	0.065
5.5	200	1.57	2	8	29	−32	0.062

[a] pH of the buffer used. At I < 100 mM, pH ≥ 4, the addition of MoA (4 mM) decreases the pH of the detergent solution by ~1 unit. [b] Mean aggregation number at $D_t = 4$ mM. [c] Standard chemical transfer potential for $N = \bar{N}$ at $D_t = 4$ mM. [d] Onset concentration of micelle formation (see text).

Hence, this onset point of the transition can be determined alternatively by linear extrapolation of the basis line and the raising part of the experimental I_3/I_1 dependencies.

Determination of the Aggregation Number Using Time-Resolved Fluorescence Measurements. The mean number of pyrene molecules per micelle, $\bar{n}$, was obtained by fitting the theoretical intensity profile[4,11,26]

$$I(t) = I_0 \exp\{-k_0 t + \bar{n}[\exp(-k_{ex} - 1)]\} \qquad (18)$$

to the fluorescence decay curves of the pyrene monomers in the micellar dispersion (Figure 8). The rate constants k_0 and k_{ex} refer to the monomer fluorescence and to the excimer formation, respectively.

Using eq 16 with the approximations $f_m \approx 1$ and $D_m \approx (D_t - \text{cmc})$, one obtains a first-order relation between the mean number of pyrene molecules per micelle and the mean aggregation number, $\bar{n} = \bar{N} r_{Py} D_t/(D_t - \text{cmc})$.[11] Linear regression of the experimental data vs the argu-

(26) Almgren M.; Löfroth, J.-E. *J. Colloid Interface Sci.* **1981**, *81*, 486.

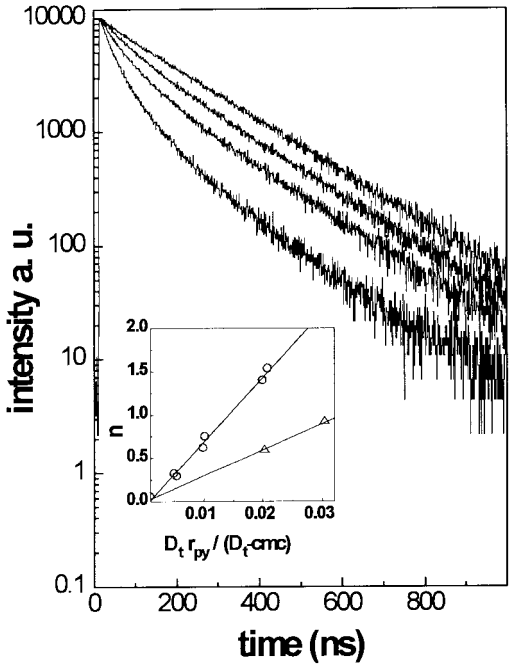

Figure 8. Fluorescence decay curves of $C_{12}EO_8$ micelles containing pyrene with r_{py}: 0.001, 0.005, 0.01, 0.05 (from top to bottom). D_t was 5 mM. The mean number of pyrene molecules per micelle, $\bar{n}$, was determined fitting eq 18 to the fluorescence decays. $\bar{n}$ vs the concentration of pyrene, C_{py} divided by D_t − cmc gives the mean aggregation number $\bar{N} = 70 \pm 4$ as the slope (○, inset). An analogous procedure gives for MoA (pH = 5.5; $I = 200$ mM) $\bar{N} = 29 \pm 3$ (△, inset).

Table 2. Mean Aggregation Number of MoA Micelles

pH	I (mM)	D_t (μM)	$\bar{N}^a$	$\bar{N}^b$
5.5	200	4000	29	
6.8	316	4000	31	29
		2000	29	28.7
		1000	29	28.5
		600	26	28.3

[a] Determined from the fluorescence decay of pyrene monomers. [b] Calculated from the polydispersity model (eq 3).

ment $r_{Py} \cdot D_t/(D_t - \text{cmc})$ yields a mean aggregation number of $\bar{N} = 70 \pm 4$ for $C_{12}E_8$ micelles (Figure 8, inset). The mean aggregation number of MoA micelles has been measured in solutions of high ionic strength at different concentrations (see Figure 8 inset and Table 2). Note that, in solutions of lower ionic strength, a considerable amount of the fluorophore remains in the aqueous phase giving rise to an intense, relatively short-lived (<50 ns) decay component which distorts the decay curve of micelle-bound monomers and, thus, prevents the analysis of the time-resolved data in terms of the decay function given above.

Discussion

Charge Number and Standard Chemical Transfer Potential. The infrared and fluorescence measurements yield two independent estimates of the apparent charge number of MoA as a function of pH, $z_{IR} = q_{max}\alpha_{MoA}(\text{pH})$ (cf. Figure 3) and the charge numbers, z_{fl}, extracted from the polydispersity model (cf. Table 1). Both data sets correlate linearly, but with a slope differing somewhat from unity (cf. Figure 9).

Whereas the IR data reflect the local extent of dissociation directly, the simple electrostatic model analyzes the effect of ionic charge on aggregation behavior and, thus, represents an indirect measure of the charge number.

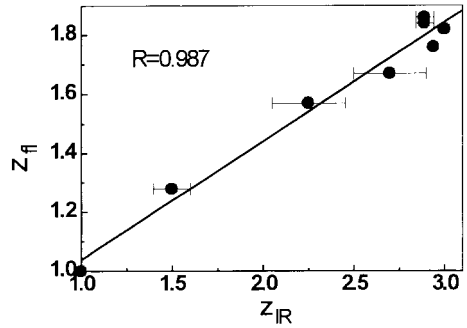

Figure 9. Correlation plot between the charge numbers determined by means of infrared and fluorescence measurements as a function of pH. The horizontal error bars indicate the pH range passed within the experiments (see footnote *a* in Table 1). The regression coefficient of the linear fit is 0.987.

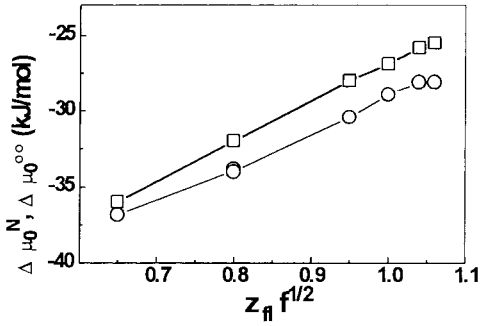

Figure 10. The standard chemical transfer potential $\Delta\mu_0^N$ and $\Delta\mu_0^\infty$ corresponding to $N = \bar{N}$ and $N \to \infty$, respectively, as a function of the effective charge number of the MoA molecules. See eqs 3 and 4 and footnotes *b* and *c* of Table 1 for definitions.

In particular, the assumption that the charged groups are located on a spherical surface represents a relatively high level of approximation. The enol group is expected to be located more distantly from the center of the micelles than the carbonyl and phosphate groups, respectively. The model used is therefore expected to overestimate the Coulombic interactions, i.e., to underestimate the apparent charge. Vice versa we conclude from the slope of the correlation plot that the enol groups are indeed exposed to the water phase at the outer surface of the micelles as suggested from pK_a measurements.

The micellization of MoA is driven by the (negative) difference between the standard chemical potentials of the detergent situated in the micelle and dissolved in water, respectively (cf. eq 4). Figure 10 shows that the chemical transfer potential, $\Delta\mu_0^N$, corresponding to micelles of mean aggregation number, i.e., $N = \bar{N}$, increases with the effective charge number, $\sim zf^{1/2}$ (cf. eq 5). Hence, micelle formation becomes less favorable upon increasing the charge of the detergent, and as a consequence, the cmc increases (Table 1). Equation 1 can be rearranged into

$$\Delta\mu_0^N = RT\left(\ln X_w^N - \frac{1}{N}\ln\frac{X_m^N}{N}\right) \qquad (19)$$

Using the approximations given by eq 2 and $D_w = \text{cmc}$ this equation transforms for the limiting case of large aggregates ($N \to \infty$) into the well-known relation of the phase separation model $\Delta\mu_0^\infty = RT \ln(\text{cmc}/W)$. Considering only the mean aggregation number, i.e., $N = \bar{N}$, and defining the cmc arbitrarily to be the aqueous detergent concentration at which the detergent distributes equally between the aqueous and micellar phases, i.e., cmc = D_w

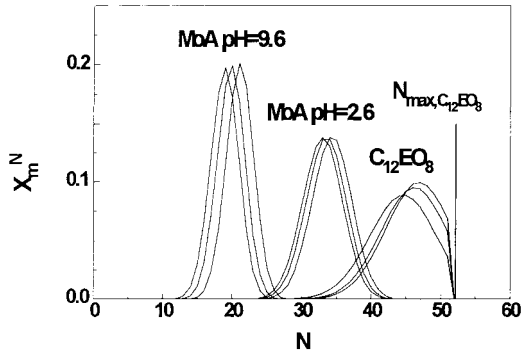

Figure 11. Mole fraction of the detergent situated in micelles of the aggregation number, N, at total detergent concentrations $D_t = 0.8$, 1.0, and 5.0 cmc: $C_{12}EO_8$ (a) and MoA (b, pH = 2.6; c, pH = 9.6).

$= D_m = 0.5D_t$, one can rewrite eq 19 as

$$\Delta\mu_0^N = \Delta\mu_0^\infty - \frac{1}{N}(\Delta\mu_0^\infty - RT \ln N) \qquad (20)$$

This relation shows that $\Delta\mu_0^\infty$ in general underestimates the absolute value of the chemical transfer potential because it does not take account of the mixing entropy of the micelles in the dispersion. For MoA, one obtains a systematic deviation of 0.8−2.5 kJ/mol (see Figure 10). The bigger values correspond to the smaller aggregation numbers. For the $C_{12}E_8$ micelles, the difference amounts to 0.7 kJ/mol.

Mean Aggregation Number and Polydispersity. The data treatment in the frame of the polydispersity model implies the calculation of the size distribution of micelles existing at a given detergent concentration. In general, the mean aggregation number of the micelles increases with increasing D_t (see Figure 11). For MoA we obtained good agreement between the mean aggregation numbers calculated from the polydispersity model and the values that were measured directly using the fluorescence decays of pyrene monomers (cf. Table 2). We conclude that MoA forms small spherical micelles, the aggregation number of which increases when the effective charge of the MoA molecules decreases. In the pH range investigated, $\bar{N}$ changes by nearly a factor of 2 from 21 up to 36 (see Table 1). A spherical shape is quite reasonable for MoA micelles because, for surfactants with a large headgroup such as MoA, a spherical shape actually is the most probable average structure. In general, one has to consider that the micelle system is perturbed by the incorporation of the pyrene probe. The tendency of pyrene to incorporate into small micelles can be thought to reduce the cmc slightly and to increase the mean aggregation number due to the hydrophobic nature of the fluorescent probe. Preliminary demicellization experiments using isothemal titration calorimetry (ITC) confirm the cmc values of MoA at pH = 2.6 and pH = 9.6, i.e., at the lowest and highest pH used in the fluorescence investigations (unpublished results). Because ITC does not involve any system perturbation, we conclude that the properties of the aqueous MoA dispersions are not affected significantly by the probe molecules.

In contrast to MoA, the size distribution of $C_{12}E_8$ is asymmetrically shaped at detergent concentrations above the cmc, and furthermore, the corresponding mean aggregation number of ∼50 is significantly smaller than that which has been measured directly ($\bar{N} = 70$). Equation 9 yields an upper limit of $N_{max} = 56$ for spherical micelles of amphiphiles with dodecyl chains ($n_h = 12$). Note, that $N = 56$ is just about the abscissa value where the right flank of the size distribution approaches zero. Obviously, the assumption of spherical micelles is in contradiction to the mean aggregation number measured directly, indicating possibly a nonspherical form of $C_{12}E_8$ micelles. Due to the synthesis, ethylene oxide surfactants such as $C_{12}E_8$ are not strictly monosized. This effect potentially increases the width of the size distribution of the micelles slightly. For MoA, the mean aggregation number remains clearly smaller than $N_{max} = 89$, and thus, the assumption of spherical micelles seems to be justified.

Fluorescent Probes for Micelle Formation. Fluorescence probe techniques combine properties of the probe molecules with that of the matrix. We demonstrated that pyrene is more suited to investigate aggregation phenomena in aqueous solution than DPH. Probably, the latter molecule partitions less into the micelles of MoA, as indicated by the continuous intensity increase with increasing MoA concentration. On the other hand, pyrene shows characteristic breakpoints in the course of two intensity ratios correlating with micelle formation. Micelle properties (size, size distribution, surface charge) depend on the detergent used and the external conditions (pH, ionic strength, detergent concentration). A variation of micelle properties is expected to modify the distribution of the fluorescent probes between the aqueous and micellar phases on the one hand and to change their fluorescence emission properties on the other hand. Our data treatment includes the partition coefficient of the probe, P, and the effective excimer formation constant, K, as free adjustable parameters.

For MoA micelles, the P values of pyrene decrease by more than 1 order of magnitude when the aggregation number decreases from ∼36 to ∼21 (Table 1). In other words, pyrene incorporates much more into bigger, noncharged micelles than into smaller, charged ones.

The variation of the partition coefficient, P, can be interpreted as an indication of structural changes of aggregates. A modification of the molecular packing of MoA in micelles of different size would affect the partition coefficient and the excimer formation rate as well. Possibly, the higher K and smaller P values reflect a looser molecular packing within the charged, smaller micelles. However, the polarity sensitive intensity ratio $I_3/I_1 \approx 0.85$ is nearly constant in all MoA systems investigated at $D_t \gg$ cmc (Figure 6), and thus, the probe environment seems to remain almost unchanged.

The corresponding parameters of $C_{12}E_8$ micelles are $P = 2.5 \times 10^6$ and $K = 18$. P adopts a value similar to that of MoA at low pH or high ionic strength, i.e., at conditions where the cmc of MoA and $C_{12}E_8$ also appear in a similar concentration range <0.1 mM.

Pyrene excimer formation has been treated using the local concentration of pyrene monomers at a given external condition (eq 15). A more exact calculation should take into account the distribution of pyrene molecules between the micelles according to Poisson statistics. This requires an additional summation over micelles containing different numbers of pyrenes. We found that this refinement gives rise to small systematic shifts of the fit parameters below the level of significance. The computational time increases, however, drastically and therefore we prefer the simpler data treatment given above.

Conclusions

In aqueous solution, MoA forms small, spherical micelles the cmc of which varies by ∼1 order of magnitude with changing pH and ionic strength. The dissociation of the

glyceric acid carboxyl and enol groups and the charged phosphate moiety account for the variability of the aggregation behavior. These properties should be taken into account in investigations on MoA membrane interactions because the effective concentration of the antibiotic within the bilayers is expected to depend essentially on the monomer concentration in the aqueous phase. Furthermore, the effective charge of MoA could modify the incorporation of the antibiotic into the membranes.

Generally, fluorescent probe techniques are well suited to investigate the micelle formation of detergents. However, the sensitivity of a hydrophobic fluorescent molecule to detergent aggregation can vary over a wide range. Pyrene fluorescence has been found to reflect micelle formation under all conditions investigated in this study whereas DPH is not appropriate for the ionic MoA. Plots of the intensity ratios of pyrene fluorescence I_3/I_1 and I_{ex}/I_{mo} vs the total detergent concentration show characteristic breakpoints which quantify the cmc. Furthermore, the fluorescence data can be analyzed in terms of a simple model which considers polydispersity of micelles and electrostatic interactions between the detergent molecules as well as emission properties of the probe and their distribution between the aqueous and aggregated phases. This model seems to reflect system properties adequately with respect to the charge number of MoA and the mean aggregation number as has been proven by independent FTIR and time-resolved fluorescence measurements. We expect that the model can be extended in principle to nonspherical aggregates in order to achieve agreement with structural parameters obtained for micelles of the nonionic detergent $C_{12}E_8$.

Acknowledgment. This work was supported by the Deutsche Forschungsgemeinschaft (INK 23, SFB 294). We thank Professor A. Blume for relevant advice and Ms. U. Dietrich and Ms. R. Herold for excellent technical assistance.

LA980214I